Application of novel low-intensity non-scanning fluorescence lifetime imaging microscopy for monitoring excited state dynamics in individual chloroplasts and living cells of photosynthetic organisms

Hann-Jörg Eckert[a], Zdeněk Petrášek[b] and Klaus Kemnitz[b]

[a]Max-Volmer-Laboratory for Biophysical Chemistry, Technical University Berlin, Straße des 17. Juni 135, D-10623 Berlin, Germany;
[b]Europhoton GmbH, Berlin, Mozartstraße 27, D-12247 Berlin, Germany

ABSTRACT

Picosecond fluorescence lifetime imaging microscopy (FLIM) provides a most valuable tool to analyze the primary processes of photosynthesis in individual cells and chloroplasts of living cells. In order to obtain correct lifetimes of the excited states, the peak intensity of the exciting laser pulses as well as the average intensity has to be sufficiently low to avoid distortions of the kinetics by processes such as singlet-singlet annihilation, closing of the reaction centers or photoinhibition. In the present study this requirement is achieved by non-scanning wide-field FLIM based on time- and space-correlated single-photon counting (TSCSPC) using a novel microchannel plate photomultiplier with quadrant anode (QA-MCP) that allows parallel acquisition of time-resolved images under minimally invasive low-excitation conditions. The potential of the wide-field TSCSPC method is demonstrated by presenting results obtained from measurements of the fluorescence dynamics in individual chloroplasts of moss leaves and living cells of the chlorophyll *d*-containing cyanobacterium *Acaryochloris marina*.

Keywords: FLIM, fluorescence lifetime, chloroplasts, photosynthesis, Chlorophyll *d*, *Acaryochloris marina*

1. INTRODUCTION

Photodynamic reactions are a common phenomenon encountered in standard fluorescence microscopy, especially in scanning confocal systems where average and peak powers are very high, causing photobleaching and photoconversion. Even in the absence of apparent bleaching, photodynamic reactions can occur during image acquisition, and are revealed only by changes in fluorescence dynamics parameters, such as lifetimes and preexponential factors. Photodynamic reactions, such as those observed with popular fluorescence probes acridine orange,[1] GFP[2,3] and YFP[4,5] may lead to wrong interpretations of the results of the experiment. For example, in fluorescence resonance energy transfer (FRET) studies, where a change of emission wavelength is usually interpreted as indication of energy transfer, photodynamic transformation of the green GFP into a red variant can be falsely identified as FRET.[3] While the mechanisms of photoconversion are often not known, photodynamic effects in photosynthetic systems are rather well understood, and involve singlet-singlet annihilation, closing of reaction centres or photoinhibition[6,7]. In order to avoid photodynamic reactions, a minimally invasive system that can operate at the 1–10 mW/cm^2 excitation level is required. The wide-field non-scanning TSCSPC method[8] using imaging quadrant anode microchannel plate photomultipliers (QA-MCP-PMT)[9] can be applied to investigation of living cells and fluorescence lifetime imaging (FLIM) without inducing significant photodynamic reactions, and while keeping the cells in their native state. In the present work we apply this technique to the investigation of fluorescence dynamics in living cells of the chlorophyll *d*-containing cyanobacterium *Acaryochloris marina* and in individual chloroplasts of moss leaves.

Further author information: (Send correspondence to H-J. E. or K. K. (TSCSPC))
H-J. E.: e-mail: hannjorg@physik.TU-Berlin.de, Tel.: +49 30 314 21067, Fax: + 49 30 314 21122
Z. P.: e-mail: zdenek.petrasek@biotec.tu-dresden.de, present address: Institut für Biophysik / Biotec, Technische Universität Dresden, Tatzberg 47–51, 01307 Dresden, Germany
K. K.: e-mail: kkemnitz@t-online.de, Tel.: +49 30 771 90145, Fax: +49 30 771 4450

Advanced Photon Counting Techniques, edited by Wolfgang Becker, Proc. of SPIE
Vol. 6372, 637207, (2006) · 0277-786X/06/$15 · doi: 10.1117/12.685958

The chlorophyll fluorescence is mainly emitted by the light harvesting antenna of Photosystem II (PS II), which in higher plants and most cyanobacteria consists mostly of chlorophyll *a* (Chl *a*) and Chl *b* molecules. After light absorption by the chlorophylls of the antenna system of PS II the electronic excitation migrates via singlet-singlet energy transfer to the reaction center, where it induces a primary charge separation between the primary donor P680, a special Chl *a* molecule, and the primary pheophytin (Pheo) acceptor forming the radical pair $P680^{+}Pheo^{-}$. The fluorescence lifetime depends not only on the radiative and non-radiative decay channels of the excited singlet state of Chl *a* (Chl a^{*}), but also on the trapping of electronic excitation by the reaction center of PS II and subsequent charge separation.[10] Measurements of fluorescence dynamics at low excitation intensity therefore provide a valuable non-invasive tool for analyzing transfer of excitation energy and primary electron transfer in PS II of photosynthesizing organisms.[10]

The cyanobacterium *A. marina* discovered only in 1996 is unique among other photosynthesizing organisms because it contains chlorophyll *d* (Chl *d*) as the major photosynthetic pigment, as opposed to the usually dominant Chl *a*. The Q_y absorption band of Chl *d* is shifted by 30 nm towards longer wavelengths with respect to Chl *a*[11] . This enables *A. marina* to utilize the light above 700 nm and to live in an environment with extremely low light level, where most of the visible light has been absorbed by other Chl *a*-containing cyanobacteria.[12]

2. MATERIALS AND METHODS

2.1. Experimental setup

The experimental setup is depicted in Fig. 1. The sample was illuminated with a 635 nm pulsed diode laser (Pilas 635, Advanced Photonics Systems, Berlin) producing an average light intensity on the sample of less than 9 mW/cm^2; the pulses were 40 ps long, at frequency 1 MHz. The emitted light was collected with a 100x oil immersion objective (Planapo, NA 1.3, Leica), and separated from the excitation light by a dichroic beamsplitter (Chroma Q660LP). Scattered excitation light was eliminated by a combination of 665 nm and 695 nm glass longpass filters. The sample was imaged by the microscope optics onto the photocathode of the quadrant anode (QA) microchannel plate photomultiplier of the TSCSPC system (Europhoton GmbH, Berlin).

2.2. TSCSPC method and QA detector

The non-scanning TSCSPC method, developed by EuroPhoton GmbH during the past 10 years,[8] is an imaging variant of well-known time-correlated single photon counting (TCSPC).[13] TSCSPC is a multi-parameter recording system that can simultaneously acquire x and y coordinates, TAC time, absolute arrival time, polarization, and wavelength information of the detected photon. The present quadrant anode detector is an improved version of the original concept[14] and represents an imaging photon-counting device with time resolution of down to approximately 15 ps after deconvolution (150 ps FWHM IRF). The photon impinging on the photocathode generates a photoelectron which is further amplified by two multichannel plates (MCP). The resulting electron cloud is accelerated towards the anode divided into four quadrants and surrounded by a fifth, auxiliary electrode. Due to the distance between the second MCP and the anode, the electron cloud spreads to some degree before hitting the anode, and consequently all five anode elements collect a certain charge. Since the position of the center of the electron cloud is determined by the original position where the photon hit the photocathode (and where the image of the sample is formed), the five measured charges reflect this position. A dedicated algorithm integrated in the control software of the QA calculates the position of every detected photon from the charges and thus reconstructs the image.

The precise timing of every photon is achieved by TCSPC[13] using a signal from one of the MCPs as a start pulse, and a synchronization signal from the pulsed excitation laser provided by a fast photodiode as a stop pulse for the time-to-amplitude converter (TAC). In the presented work a temporal window of 20 ns divided into 4096 channels was used, allowing accurate fluorescence decay analysis. In addition to this fast TAC time, absolute timing of every photon relative to the start of the measurement ('absolute arrival time') is provided by means of a 12.5 MHz clock (i.e., with 80 ns resolution). This information can be used to divide a long measurement into smaller parts and analyze those individually in order to monitor the temporal evolution of the sample. Additionally, the high temporal resolution of this 'absolute arrival time' can in principle be exploited to perform offline correlation analysis of the signal in different parts of the sample (spatially resolved fluorescence correlation spectroscopy).

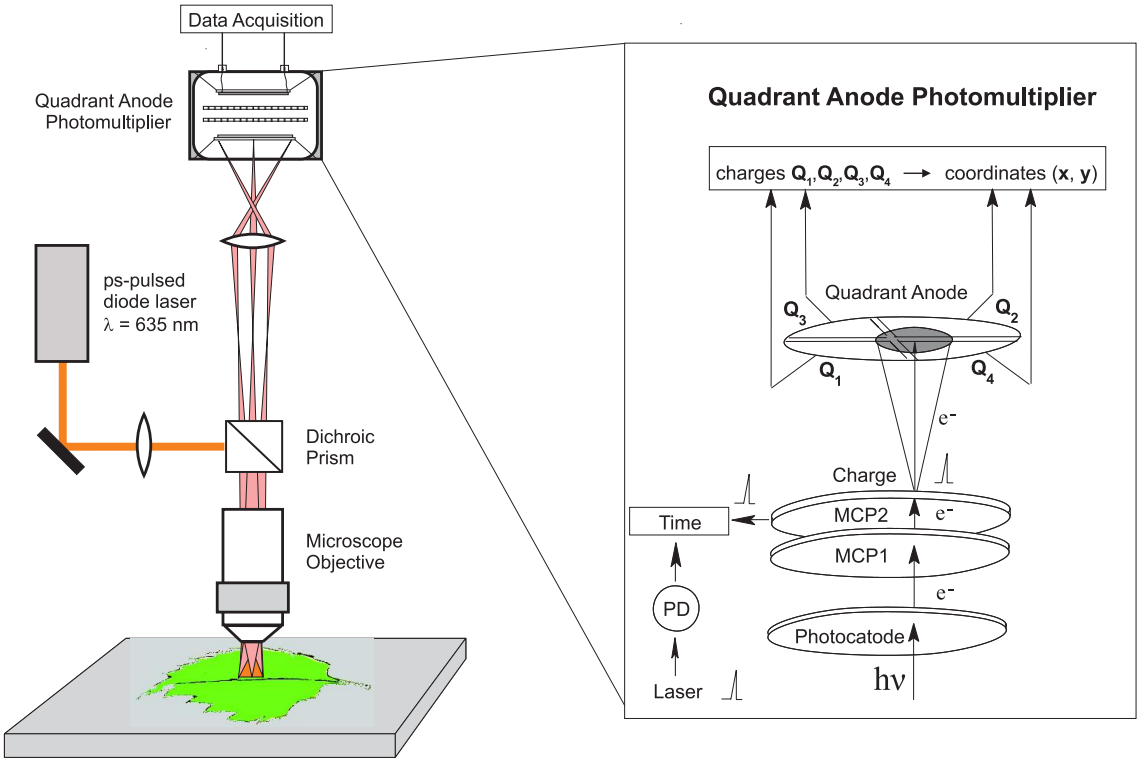

Figure 1. Scheme of the FLIM setup (left) and of the QA-detector (right)

The raw data produced by the QA detector consist of a stream of records ('list mode'), each containing several values describing the detected photon: two spatial coordinates (x, y), the TAC time (the arrival time relative to the excitation pulse) used for fluorescence decay reconstruction, the 'absolute arrival time' (the time relative to the start of the measurement), and, optionally, polarization and wavelength information. The file size easily reaches hundreds of megabytes and depends on the total number of photons, i.e., on the time of the measurement and the average fluorescence intensity. Since complete information about every photon is preserved, the raw data can be processed and analyzed in many different ways.

2.3. Sample

A. marina was grown as described by Chen *et al.*[15] in artificial sea water at 28 ± 2°C under an illumination intensity of about 0.5 mW/cm^2 and continuous aeration. The suspension of *A. marina* cells in the growth medium was enclosed in a 10 μm deep well covered with a coverslip and placed on a microscope stage. The concentration of the cellular suspension was chosen so that sufficient number of non-overlapping cells was present in the field of view. The small depth of the observation well ensured that the motion of the cells due to convection currents during the long measurement periods (up to one hour) was minimized, although it could not be eliminated altogether. The sample was dark-adapted for five minutes prior to the measurement.

2.4. Data analysis

The measurement presented here lasted 67.5 minutes, and was divided into 3 blocks of equal length (1350 s) for analysis. Fluorescence intensity and lifetime images were constructed from each block of data. The field of view was divided into 256x256 pixels. The number of photons falling into a given pixel defined its intensity (fluorescence image), and the temporal distribution of these photons (fluorescence decay), determined from the 'TCSPC' times, was used to calculate the lifetime image. The lifetime in every pixel was estimated by fitting the fluorescence decay to a monoexponential function. The fitting was performed in the temporal range defined

by the time channel of the maximum intensity and the channel where the recorded intensity reaches zero value. Pixels with photon counts lower than a defined threshold value were excluded from the lifetime images due to the too low signal-to-noise ratio.

In order to increase the signal-to-noise ratio, fluorescence decays were extracted from defined regions of interest, in this case the whole *A. marina* cells. The decays were analyzed by iterative reconvolution with the Levenberg-Marquardt algorithm used for χ_r^2 minimization.[13] The model for the decay of fluorescence $F(t)$ following a short excitation pulse was a sum of one to three exponentials:

$$F(t) = \sum_{i=1}^{3} a_i e^{-t/\tau_i}. \quad (1)$$

In some cases, global fit of several fluorescence decays was performed, whereby the lifetimes τ_i were common to all decays and the preexponential factors a_i were optimized for every decay independently. The mean lifetime of a decay was calculated as an average of the lifetimes τ_i weighed by the preexponential factors a_i.

The instrument response function (IRF) was measured by detecting a reflection of an attenuated excitation beam from a mirror placed in the object plane of the microscope. The complex analysis involving convolution with IRF was not employed while calculating lifetime images due to the weaker signal in single-pixel decays. Not taking into account the effects of the finite IRF in the FLIM analysis results in small systematic differences between the lifetimes in FLIM images and the mean lifetimes in extracted decays.

3. RESULTS

3.1. *A. marina* cells

For a comparison with the fluorescence measurements in individual cells of *A. marina* described below, Fig. 2 shows the results of time- and wavelength-resolved fluorescence measurements in a large ensemble of cells. These measurements were performed with the equipment described by Bergmann *et al.*[16] The fluorescence spectrum (Fig. 2, left) is characterized by two bands at about 650 nm and 725 nm. The 650 nm fluorescence is ascribed to emission from phycocyanin (PC) and allophycocyanin (APC) of the phycobiliprotein antenna of *A. marina*[17,18]. The 725 nm fluorescence originates from Chl *d* of Photosystem I (PS I) and PS II[17,19]. The kinetics of the fluorescence decay depends strongly on the emission wavelength with a much shorter lifetime at 660 nm than at 725 nm (Fig. 2, right). The 650 nm fluorescence decays predominantly with a lifetime of about 70 ps reflecting fast energy transfer from APC to Chl *d*.[17] In contrast, the 725 nm fluorescence can be described by a three-exponential decay kinetics with lifetimes of about 100 ps, 600 ps and a slow component with a lifetime of about 1.5 ns. The fast 100 ps component is ascribed to Chl *d* of PS I while the middle and the slow components are due to Chl *d* of PS II.[17]

The ensemble fluorescence measurements described above provide only the fluorescence kinetics averaged over a large number of cells. In order to obtain information about the fluorescence dynamics in individual cells, measurements were performed using the FLIM setup described in the Materials and Methods section. The results are summarized in Fig. 3. Since a 695 nm long-pass emission filter was used during these measurements, the detected fluorescence was mainly due to Chl *d* and not PC or APC emission. Fig. 3a depicts the spatial distribution of the fluorescence photons accumulated during the measurement. The bright spots represent the fluorescence emitted from individual cells of *A. marina*. For each cell, the corresponding fluorescence decay curve can be constructed from the time and space information of every detected fluorescence photon stored in the computer (see Materials and Methods). Typical fluorescence decay curves of two individual cells (no. 4 and no. 7) are shown in Fig. 3b together with the instrument response function (IRF) of the equipment.

The fluorescence decays of the ten individual cells marked in Fig. 3a were analyzed globally according to eq. 1 with common values of lifetimes (linked parameters) and cell-dependent pre-exponential factors a_i. In good agreement with the ensemble measurements shown in Fig. 2 the fluorescence decay in the ten cells is characterized by two main components with lifetimes of $\tau_{\text{fast}} = 60$ ps and $\tau_{\text{middle}} = 800$ ps and a slow component with lifetime of about $\tau_{\text{slow}} = 1.6$ ns. The pre-exponential factors for the different cells are plotted in Fig. 3e. The main feature is a large variation in the relative contribution of the slow component. It is practically 0% in cells no. 2,

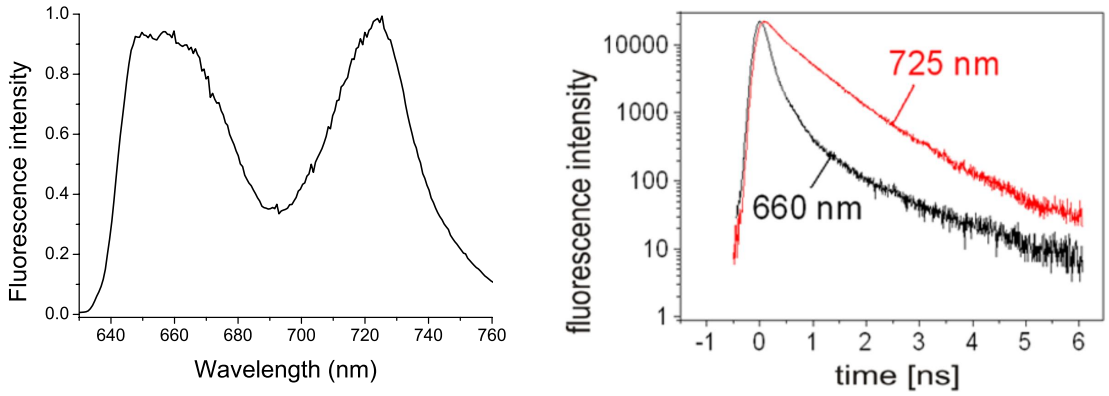

Figure 2. Fluorescence spectrum (left) and normalized fluorescence decays at 725 nm and 660 nm in a large ensemble of whole cells of *A. marina* at 25°C. In the short wavelength range the spectrum is affected by a long-pass emission filter (640ALP, Omega Inc.) with a cut off wavelength of 640 nm.

3, and 4 and has increased values of up to nearly 25% in some cells (no. 7, 9 and 10). Larger contribution of the slow 1.6 ns component is generally connected with decreased amplitude of the 800 ps component. In contrast, within the experimental error, the contribution of the fast 60 ps component shows nearly the same value in all cells.

Based on the ensemble measurements presented in Fig. 2 the fast decay component is assigned to Chl *d* fluorescence from PS I which is known to have a very short fluorescence lifetime[17,19]. The other two decay components originate from Chl *d* of PS II.[17] The middle component is assigned to PS II with so called "open" reaction centers with oxidized plastoquinone acceptor QA, while the slow decay component is known to be a characteristics of PS II systems with so called "closed" reaction centers[10,17] with reduced Q_A^- (state: P680 Pheo Q_A^-). Therefore, the large contribution of the slow 1.6 ns component in cells no. 7, 9 and 10 is an indication that these cells contained a relatively large fraction of reaction centers in the closed state in spite of the relatively low excitation intensity.

For a fast survey over all cells in Fig. 3a fluorescence lifetime images (FLIM) were constructed from the time and space information of the fluorescence photons stored in the computer by single exponential fits of the fluorescence decays. The middle panels of Fig. 3 show the FLIM of the data accumulated during the first 22.5 min. (panel c) and the last 22.5 min. (panel d) of a measurement 67.5 min. long. Because of different fitting procedure applied to lifetime images (see Materials and Methods), the contribution of the fast component to the effective lifetime recovered from monoexponential fits is estimated to be rather small. Therefore, the calculated lifetime can be regarded as close to the mean lifetime of the two slow components of the fluorescence decay which are attributed to PS II. During the first measurement period (Fig. 3c) the majority of the cells had a mean lifetime below 1.2 ns and only a few cells exhibited a mean lifetime above 1.4 ns. In the last measuring period (Fig. 3d), however, most cells exhibited a lifetime above 1.2 ns and also the number of cells with a lifetime above 1.4 ns strongly increased. In order to demonstrate the changes in the decay kinetics with illumination time for a single cell, the fluorescence signal from the entire measurement of cell no. 1 was divided into 30 parts, each lasting 135 s. The fluorescence decays from the first (blue) and the last (red) part of the measurement are plotted in Fig. 3f.

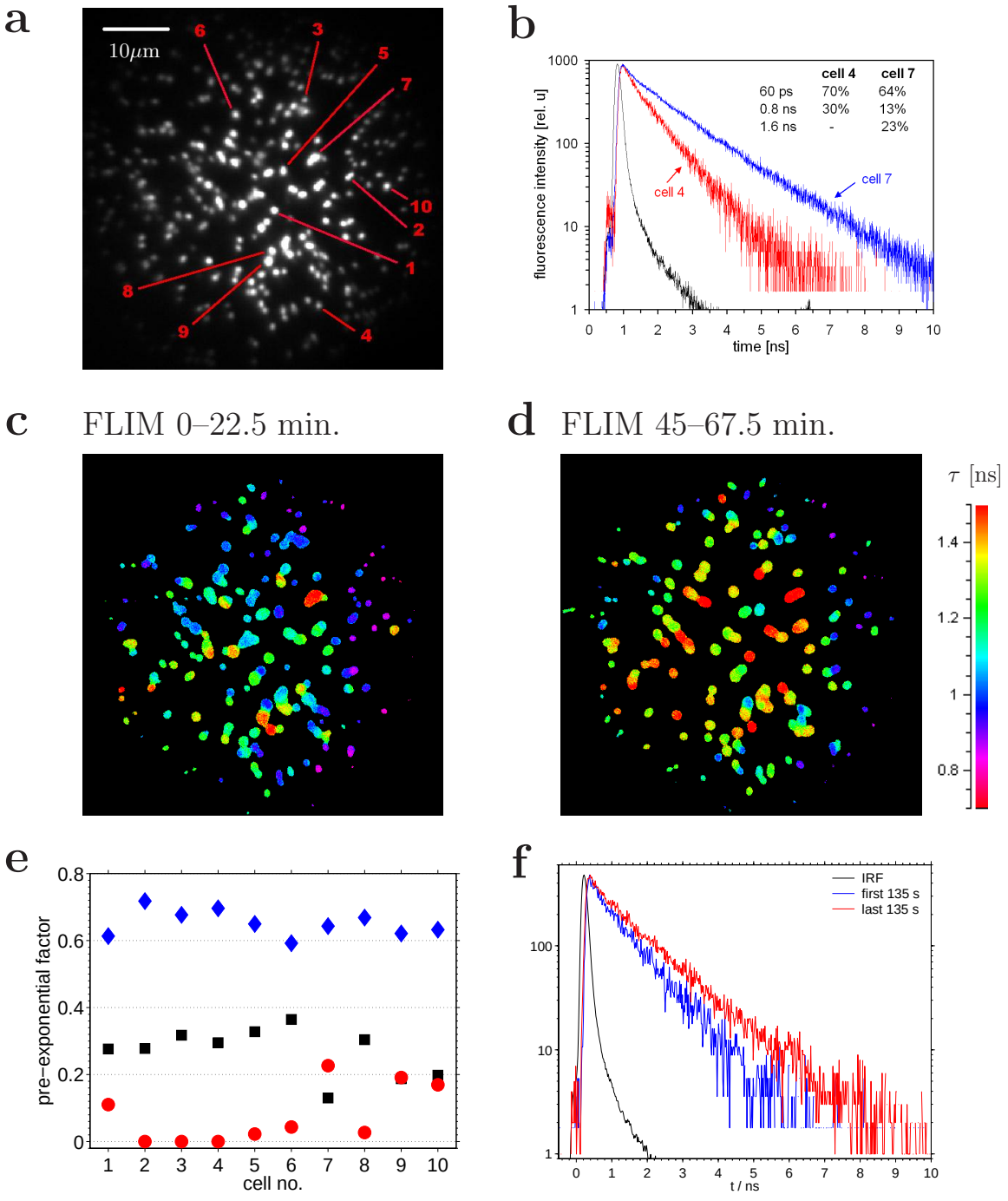

Figure 3. Fluorescence dynamics in individual cells of *A. marina*. a: time integrated fluorescence image; b: fluorescence decays in cells no. 4 and 7 extracted from the data shown in panel a; c and d: fluorescence lifetime images (FLIM) of *A. marina* constructed from the data accumulated during the first 22.5 min. (c) and the last 22.5 min. (d) of the measurement lasting 67.5 min. in total; e: pre-exponential factors a_i of the lifetime components (τ_1 = 60 ps ♦, τ_2 = 800 ps ■, τ_3 = 1.6 ns ●) obtained from a three-component global fit with linked lifetimes of the fluorescence decays in the ten cells marked in the panel a; f: fluorescence decays in cell no. 1 during the first 135 s (blue) and the last 135 s (red) of the 67.5 min. measurement.

3.2. Moss leaves

Fig. 4 shows a fluorescence lifetime image (middle) of a moss leaf obtained at a spatial resolution of about 1 μm together with a picture (left) of the same area of the leaf taken in transmission by a CCD camera. Typical fluorescence decay curves of two individual Chloroplasts (no. 8 and no. 3) are shown in the right panel. The fluorescence decays of 15 individual chloroplasts were analyzed globally (data not shown). As in the case of *A. marina*, the data could be fitted well with a three-exponential decay model. In a good agreement with measurements of suspensions of thylakoids and PS II membrane fragments,[20] the fluorescence decays are characterized by two main components with lifetimes below 500 ps (140 ps and 350 ps) and a slower component with a lifetime of about 1.2 ns. In most chloroplasts the contribution of the slow component to the initial amplitude was below 2%. In only one of the 15 chloroplasts (no. 3) the contribution of the 1.2 ns component was much larger (about 10% of the initial amplitude).

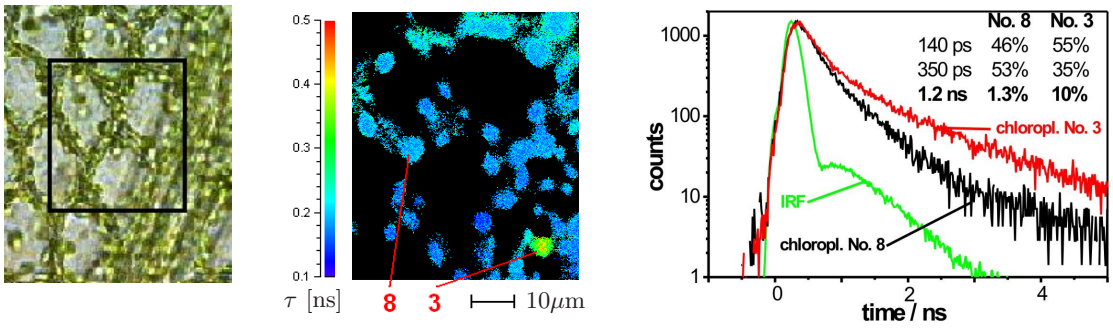

Figure 4. Fluorescence dynamics in individual chloroplasts of moss leaves. CCD-image (left), FLIM (middle) of the marked area in the CCD image and fluorescence decay in two chloroplasts (right).

4. DISCUSSION

The presented data demonstrate that the described measurement system allows simultaneous acquisition of time-resolved fluorescence data from a large number of organelles and whole cells. Measurement times as short as 2 min. (Fig. 3f) are sufficient for determination of lifetimes of individual cells at excitation light intensity lower than 9 mW/cm^2 in the sample.

The presented FLIM measurements of individual cells of *A. marina* show that the mean fluorescence lifetime of the cells varied between approximately 0.8 and 1.5 ns and that the number of cells with a long lifetime increases with the measurement time (Fig. 3). The mean lifetime of the fluorescence decay is a (non-linear) measure of the fraction of PS II reaction centers in the "closed" state with reduced plastoquinone acceptor Q_A^-. Therefore, the above findings indicate that the fraction of "closed" PS II reaction centers increases with the measurement time due to the illumination of the cells by the excitation laser beam. This is in agreement with Fig. 3c showing that the density of cells with long mean lifetime is smaller on the periphery of the illuminated area where the light intensity of the laser beam is lower. However, Fig. 3 also shows that the process of closing of the reaction centers does not only depend on the light intensity. Even cells located near each other, and therefore exposed to very similar light intensities, may exhibit quite different fluorescence lifetimes. The reason for these differences is presently not clear and is subject to further investigations. One might speculate that this effect is due to different development states of the cells, which could be connected to varying sizes of the light harvesting system. Furthermore, it has to be taken into consideration that with the used laser (λ_{ex} = 635 nm) mainly the phycobiliprotein antenna is excited. The phycobiliprotein antenna has been shown to disconnect from PS II under stress conditions, thereby leading to decreased excitation energy transfer from the PBP antenna to PS II. In contrast to the *A. marina* cells, the fluorescence decay kinetics of the chloroplasts in the moss leaf showed only slight variations, with exception of one chloroplast. In this case, the PS II reaction centers in most of the chloroplasts remained in the open state with lifetimes below 500 ps. This difference compared to *A. marina* is

understandable, if one considers that the light intensity at the samples was about 9 mW/cm^2, corresponding approximately to the natural light intensity for moss leaves, while it was rather high for the cyanobacterium *A. marina*, normally growing at very low light intensity of typically 0.5 mW/cm^2, or less.

Regardless of the details of the data interpretation, the above results demonstrate the capability of the presented wide-field, non-scanning TSCSPC fluorescence lifetime microscope. It allows investigation of the fluorescence dynamics of individual living cells at average light intensity at the sample of less than 10 mW/cm^2 without inducing significant detrimental photodynamic reactions, and determination of fluorescence lifetimes of a large number of individual organelles with sufficient quality in measuring times as short as 2 minutes.

ACKNOWLEDGMENTS

We would like to thank Franz-Josef Schmidt for providing the data of the ensemble measurements of Fig. 2, Monika Weß and Sabine Kussin for cultivating *A. marina* and Dr. Min Chen and Prof. Anthony Larkum for helpful discussions. We further thank Prof. Hans Joachim Eichler, Prof. Gernot Renger and Christoph Theiss for their support. This research has been supported by Marie Curie Fellowship (Z. P.) of the European Community programme "Quality of Life" under the contract number QLK2-CT-200-60076 and by the Deutsche Forschungsgemeinschaft (SFB 429, TP A1).

REFERENCES

1. J. Delic, J. Coppey, H. Magdelenat, and M. Coppey-Moisan, "Impossibility of acridine orange intercalation in nuclear DNA of the living cell," *Exp. Cell Res.* **194**, pp. 147–153, May 1991.
2. M. B. Elowitz, M. G. Surette, P. E. Wolf, J. Stock, and S. Leibler, "Photoactivation turns green fluorescent protein red," *Curr. Biol.* **7**, pp. 809–812, Oct. 1997.
3. T. M. H. Creemers, A. J. Lock, V. Subramaniam, T. M. Jovin, and S. Volker, "Photophysics and optical switching in green fluorescent protein mutants," *Proc. Natl. Acad. Sci. U. S. A.* **97**, pp. 2974–2978, Mar. 2000.
4. G. Valentin, C. Verheggen, T. Piolot, H. Neel, M. Coppey-Moisan, and E. Bertrand, "Photoconversion of YFP into a CFP-like species during acceptor photobleaching FRET experiments," *Nat. Methods* **2**, pp. 801–801, Nov. 2005.
5. G. Valentin, C. Verheggen, T. Piolot, H. Neel, T. Zimmermann, M. Coppey-Moisan, and E. Bertrand, "Photobleaching of YFP does not produce a CFP-like species that affects FRET measurements response," *Nat. Methods* **3**, pp. 492–493, July 2006.
6. Govindjee and J. Amesz, *Light Emission by Plants and Bacteria*, Cell Biology, Academic Press, November 1986. ISBN 0122943104.
7. H. J. Eckert, B. Geiken, J. Bernarding, A. Napiwotzki, H. J. Eichler, and G. Renger, "Two sites of photoinhibition of the electron transfer in oxygen evolving and tris-treated PS-II membrane fragments from spinach," *Photosynth. Res.* **27**, pp. 97–108, Feb. 1991.
8. K. Kemnitz, *New Trends in Fluorescence Spectroscopy: Applications to Chemical and Life Sciences*, ch. Picosecond Fluorescence Lifetime Imaging Microscopy as a New Tool for 3D Structure Determination of Macromolecules in Living Cells, pp. 381–. Springer Series on Fluorescence, Springer, 1 ed., June 2001. ISBN: 3540677798.
9. V. Emiliani, D. Sanvitto, M. Tramier, T. Piolot, Z. Petrasek, K. Kemnitz, C. Durieux, and M. Coppey-Moisan, "Low-intensity two-dimensional imaging of fluorescence lifetimes in living cells," *Appl. Phys. Lett.* **83**, pp. 2471–2473, Sept. 2003.
10. G. Renger, H. J. Eckert, A. Bergmann, J. Bernarding, B. Liu, A. Napiwotzki, F. Reifarth, and H. J. Eichler, "Fluorescence and spectroscopic studies of exciton trapping and electron transfer in photosystem II of higher plants," *Australian Journal of Plant Physiology* **22**(2), pp. 167–181, 1995.
11. H. Miyashita, H. Ikemoto, N. Kurano, K. Adachi, M. Chihara, and S. Miyachi, "Chlorophyll d as a major pigment," *Nature* **383**, pp. 402–402, Oct. 1996.
12. A. W. D. Larkum and M. Kuhl, "Chlorophyl d: the puzzle resolved," *Trends Plant Sci.* **10**, pp. 355–357, Aug. 2005.

13. D. V. O'Connor and D. Phillips, *Time-Correlated Single Photon Counting*, Academic Press, October 1984. ISBN 0125241402.
14. M. Lampton and R. F. Malina, "Quadrant anode image sensor," *Rev. Sci. Instrum.* **47**(11), pp. 1360–1362, 1976.
15. M. Chen, R. G. Quinnell, and A. W. D. Larkum, "The major light-harvesting pigment protein of Acaryochloris marina," *FEBS Lett.* **514**, pp. 149–152, Mar. 2002.
16. A. Bergmann, H. J. Eichler, H. J. Eckert, and G. Renger, "Picosecond laser-fluorometer with simultaneous time and wavelength resolution for monitoring decay spectra of photoinhibited Photosystem II particles at 277 K and 10 K," *Photosynth. Res.* **58**, pp. 303–310, Dec. 1998.
17. Z. Petrášek, F. J. Schmitt, C. Theiss, J. Huyer, M. Chen, A. Larkum, H. J. Eichler, K. Kemnitz, and H. J. Eckert, "Excitation energy transfer from phycobiliprotein to chlorophyll d in intact cells of Acaryochloris marina studied by time- and wavelength-resolved fluorescence spectroscopy," *Photochem. Photobiol. Sci.* **4**, pp. 1016–1022, Dec. 2005.
18. Q. Hu, J. Marquardt, I. Iwasaki, H. Miyashita, N. Kurano, E. Morschel, and S. Miyachi, "Molecular structure, localization and function of biliproteins in the chlorophyll a/d containing oxygenic photosynthetic prokaryote Acaryochloris marina," *Biochimica et Biophysica Acta — Bioenergetics* **1412**, pp. 250–261, Aug. 1999.
19. M. Mimuro, S. Akimoto, I. Yamazaki, H. Miyashita, and S. Miyachi, "Fluorescence properties of chlorophyll d-dominating prokaryotic alga, Acaryochloris marina: studies using time-resolved fluorescence spectroscopy on intact cells," *Biochimica et Biophysica Acta — Bioenergetics* **1412**, pp. 37–46, May 1999.
20. A. Napiwotzki, A. Bergmann, K. Decker, H. Legall, H. J. Eckert, H. J. Eichler, and G. Renger, "Acceptor side photoinhibition in PS II: On the possible effects of the functional integrity of the PS II donor side on photoinhibition of stable charge separation," *Photosynth. Res.* **52**, pp. 199–213, June 1997.